

Polariton condensation in an optically induced two-dimensional potential

A. Askitopoulos,^{1,*} H. Ohadi,¹ A. V. Kavokin,^{1,2} Z. Hatzopoulos,^{3,4} P. G. Savvidis,^{3,5} and P. G. Lagoudakis¹

¹*School of Physics and Astronomy, University of Southampton, Southampton, SO17 1BJ, United Kingdom*

²*Spin Optics Laboratory, St. Petersburg State University, 1 Ulianovskaya, St. Petersburg 198504, Russia*

³*Microelectronics Research Group, IESL-FORTH, P.O. Box 1527, 71110 Heraklion, Crete, Greece*

⁴*Department of Physics, University of Crete, 71003 Heraklion, Crete, Greece*

⁵*Department of Materials Science and Technology, University of Crete, Crete, Greece*

(Received 1 May 2013; revised manuscript received 18 June 2013; published 29 July 2013)

We demonstrate experimentally the condensation of exciton polaritons through optical trapping. The nonresonant pump profile is shaped into a ring and projected to a high quality factor microcavity where it forms a two-dimensional repulsive optical potential originating from the interactions of polaritons with the excitonic reservoir. Increasing the population of particles in the trap eventually leads to the emergence of a confined polariton condensate that is spatially decoupled from the decoherence inducing reservoir, before any buildup of coherence on the excitation region. In a reference experiment, where the trapping mechanism is switched off by changing the excitation intensity profile, polariton condensation takes place for excitation densities more than two times higher and the resulting condensate is subject to much stronger dephasing and depletion processes.

DOI: [10.1103/PhysRevB.88.041308](https://doi.org/10.1103/PhysRevB.88.041308)

PACS number(s): 03.75.Kk, 03.75.Gg, 71.36.+c

Strong coupling of cavity photons and quantum-well excitons gives rise to mixed light-matter bosonic quasiparticles called exciton-polaritons or polaritons.¹ Due to their photonic component, polaritons are several orders of magnitude lighter than atoms, which makes their condensation attainable at higher temperatures.^{2,3} The manifestations of polariton condensation include polariton lasing,⁴ long-range spatial coherence,^{5,6} and stochastic vector polarization.⁷ In an ideal infinite two-dimensional cavity the polariton gas is expected to undergo the Berezinsky-Kosterlitz-Thouless (BKT) phase transition,⁸ while in realistic structures, polaritons can condense in traps induced by random optical disorder² or mechanically created potentials.^{3,9} Polariton condensation has also been observed in structures of lower dimensionality^{10–13} where the structure itself acts as the trapping potential. Furthermore, the manipulation of polariton condensates by optically generated potentials has been previously shown.^{14–17} In these works the condensation process was not assisted by the optical potential but used to localize an already formed polariton condensate.

Here, we report on the manifestation of polariton condensation assisted by an optically generated two-dimensional potential. This scheme allows for the formation of a polariton condensate spatially separated from the excitation spot. Owing to the efficient trapping in the optical potential we observe a reduced excitation density threshold as well as higher coherence due to the decoupling of the condensate from the exciton reservoir. Our observation of polariton condensation nonlocal to the laser excitation profile, prior to the buildup of coherence at the excitation area on the sample,^{18,19} conclusively proves that the coherence of the polariton condensate is not associated with the coherence of the excitation beam.⁸

We used a high quality factor GaAs/AlGaAs microcavity containing four separate triplets of 10-nm GaAs quantum wells and has a vacuum Rabi splitting of 9 meV,²⁰ held at ~ 6.5 K in a cold-finger cryostat and excited nonresonantly at the first reflection minimum above the cavity stop band with a single-mode continuous-wave laser. The excitation beam profile was shaped into a ring in real space with the use of

two axicons and was projected to the microcavity through an objective lens [numerical aperture (NA) = 0.4] creating a polariton ring with a mean diameter of ~ 20 μm on the sample,²¹ which is of the order of the polariton mean free path in planar microcavities and much larger than the exciton diffusion length of the quantum wells of our sample.^{22,23} The excitation beam intensity was modulated with an acousto-optic modulator at 1% duty cycle with a frequency of 10 kHz to reduce heating.

The nonresonant excitation creates a hot electron-hole plasma, which then forms excitons. Hot excitons cool down by exciton-phonon scatterings.²⁴ When they enter the light cone they couple strongly to the cavity mode and populate the lower polariton branch on the ring. Excitons diffuse around the excitation area but due to their large effective mass they are unable to reach the center of the ring. The repulsion of polaritons from the ring-shaped exciton reservoir can be described by a mean-field ringlike trapping potential, which is approximately 1 meV deep in the center at the pumping power corresponding to the condensation threshold. Uncondensed polaritons start from the blueshifted states on the ring and ballistically expand²⁵ either towards the center or outside. Those which propagate to the center eventually collide with each other (see Fig. 1). The energy of the ensemble of polaritons is conserved by these scattering events, so that the kinetic energies of approximately half of the polaritons are reduced, while the other half have their kinetic energies increased. As a result, a fraction of the polariton gas is no more capable to escape from the trap due to the lack of kinetic energy, while the rest can easily fly away over the barriers. Further scatterings of the trapped polaritons lead to the increase of the kinetic energy of some of them so that they become able to leave the trap. By increasing the excitation power, the polariton population inside the trap builds up and a condensate forms at the center of the ring that is quickly enhanced due to final-state polariton stimulated scatterings.²⁶

Polariton emission in real space for powers greatly below threshold outlines the pump profile [Fig. 2(a)]. At the onset of condensation, photoluminescence (PL) from the center

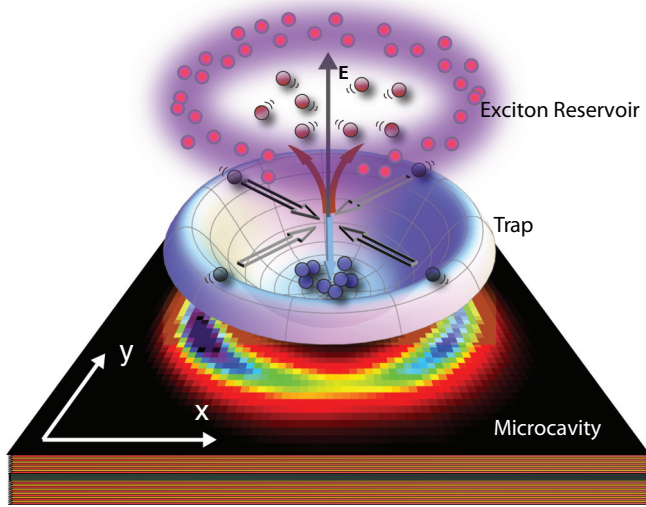


FIG. 1. (Color online) Polariton trap over real-space excitation spot, displaying the trapping mechanism. Polaritons scattered to high-energy states leave the trap, while those scattered to low energy and momentum remain confined.

of the trap is of the same intensity as emission from the ring [Fig. 2(b)]. Above threshold [Figs. 2(c) and 2(g)] a Gaussian shaped single-mode condensate, with full width at half maximum (FWHM) of $5.46 \mu\text{m}$ and standard deviation $\sigma_x = 2.32 \mu\text{m}$, is formed and effectively confined inside the ring (images of the complete power dependence have been compiled in a video that can be found in the Supplemental Material). Michelson interferometry images [inset in Fig. 2(c)] confirm the buildup of coherence in the condensate.²¹

The dispersion of polaritons for the entire surface of the ring and for different pumping powers can be seen at Figs. 2(d)–2(f). Below threshold we observe a normal lower polariton branch. As the polariton density in the center of the

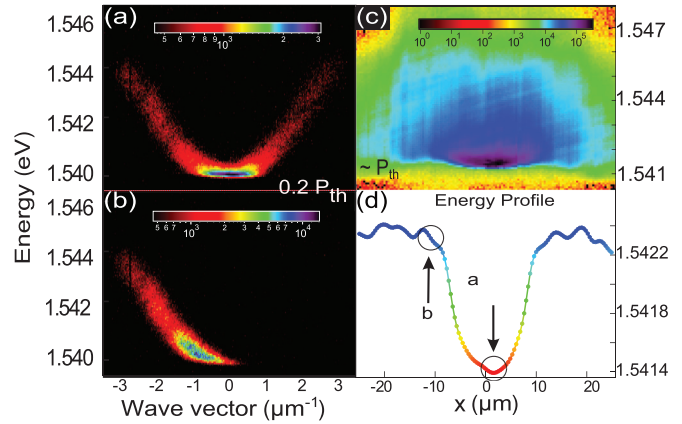


FIG. 3. (Color online) Trapping potential and spatially resolved dispersions. (a), (b) Dispersion images below threshold ($P = 0.2P_{th}$) from a $5\text{-}\mu\text{m}$ -diameter spatially filtered region from the center of the ring (a) and from the rim (b). Energy profile of the central slice of the ring at threshold (c) and the extracted maxima of intensity along the x axis for visualization of the trap profile (d). Points **a** and **b** correspond to (a) and (b) respectively.

ring is increased close to threshold, we observe a blueshifted dispersion from the polaritons in the trap, coexisting with the dispersion of untrapped polaritons as it will become evident further on, from spatially resolved dispersion imaging. The two lobes of the outer dispersion in Fig. 2(e) correspond to high momentum polaritons escaping from the center of the ring. By further increasing the excitation power a condensate appears in the ground state of the blueshifted dispersion with zero in-plane momentum and standard deviation $\sigma_{k_x} = 0.24 \mu\text{m}^{-1}$, shown in logarithmic scale in Fig. 2(f). The macroscopically occupied ground state is very close to the Heisenberg limit, having $\sigma_x \sigma_{k_x} = 0.56$ lower than previously reported values.^{27,28} This confirms that phase fluctuations in the condensate are strongly reduced.

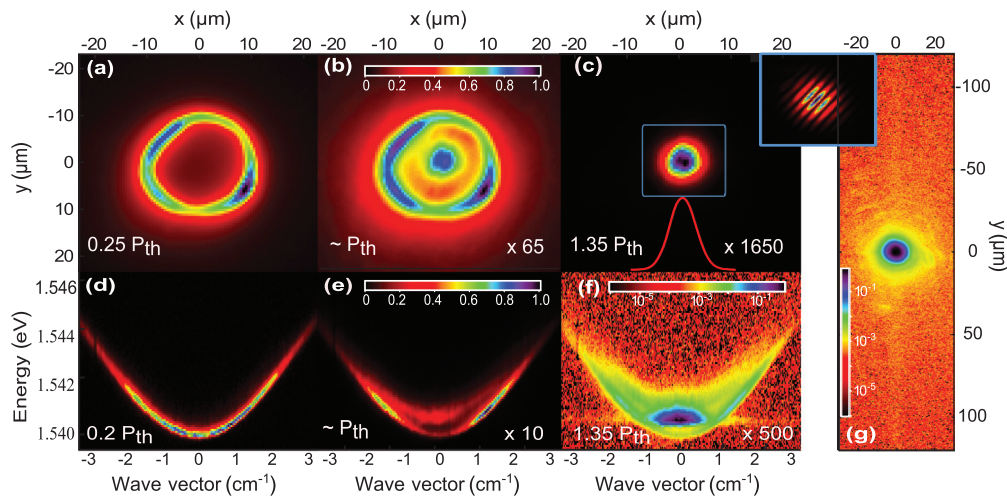


FIG. 2. (Color online) Single-mode exciton-polariton condensate in a ring-shaped trap. Emission images in real space below (a), at (b), and above threshold (c). The inset in (c) shows the interference fringes of the condensate. Red line in (c) is the condensate profile along the x axis. Polariton condensation is clearly visible in the center of the ring and is separate from the excitation spot outlined by the emission in (a). (d)–(f) Dispersion images below (d), at (e), and above (f) threshold. (g) Same as (c) but with a logarithmic color scale showing that the condensate propagation beyond the trap is minimal.

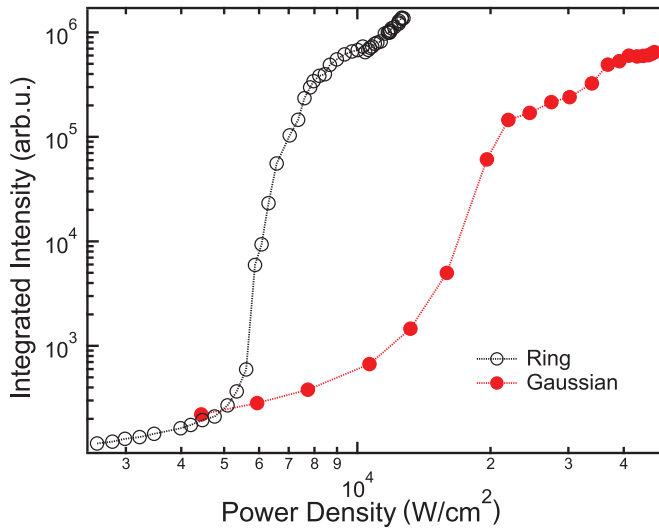


FIG. 4. (Color online) Integrated intensity with increasing power density from the trapped condensate (open black circles) and from a Gaussian excitation (red circles) measured at $k = 0 \mu\text{m}^{-1}$ of the spatially filtered dispersions.

Spatially resolved dispersion images reveal that untrapped polaritons positioned on the rim of the ring have high energies and large wave vectors [Fig. 3(b)], while those in the center of the trap primarily populate the lower states even at pump powers much below threshold [Fig. 3(a)].²¹ The dispersion of the polaritons on the edge of the ring does not change greatly with increasing power (for the power range that we examined), while the dispersion images at the center of the trap demonstrate condensation at $k = 0$ above threshold. The profile of the trap can be visualized by energy resolving a central slice ($\sim 1.3 \mu\text{m}$) of the excitation ring [Fig. 3(c)]. By extracting the energy that corresponds to the maximum intensity along each point of the x axis of Fig. 3(c), the trap potential can be assembled [Fig. 3(d)]. The trap depth at threshold is $\sim 1 \text{ meV}$. The two circles in Fig. 3(d) annotate the points where the spatially filtered dispersions were acquired.

Due to the efficient stimulated scattering process inside the optical trap, we observe significantly lower power densities for condensation. In a reference experiment we have excited the same sample (at the same detuning, -4 meV , temperature, and pump on: off ratio) with a Gaussian beam of spot size $\sim 5 \mu\text{m}$. Figure 4 shows the integrated photoluminescence (PL) intensity at $k = 0$ for different excitation powers of the two experiments. Remarkably the condensation threshold power density is found to be more than two times higher in the case of Gaussian excitation.

Full spatial separation of the condensate from the pump induced excitonic reservoir has important implications on the spectral and dynamic properties of polaritons²⁹ even below threshold. Already in the linear regime the linewidth of the trapped particles in the ground state is almost two times lower ($\sim 250 \mu\text{eV}$) compared to polaritons in the ground state injected by a beam excitation, which interact strongly with excitons from the reservoir [Fig. 5(a)]. In the nonlinear regime, a clear advantage of the decoupling of the coherent polaritons from the incoherent reservoir is the strong reduction of the depletion processes caused by the condensate-reservoir

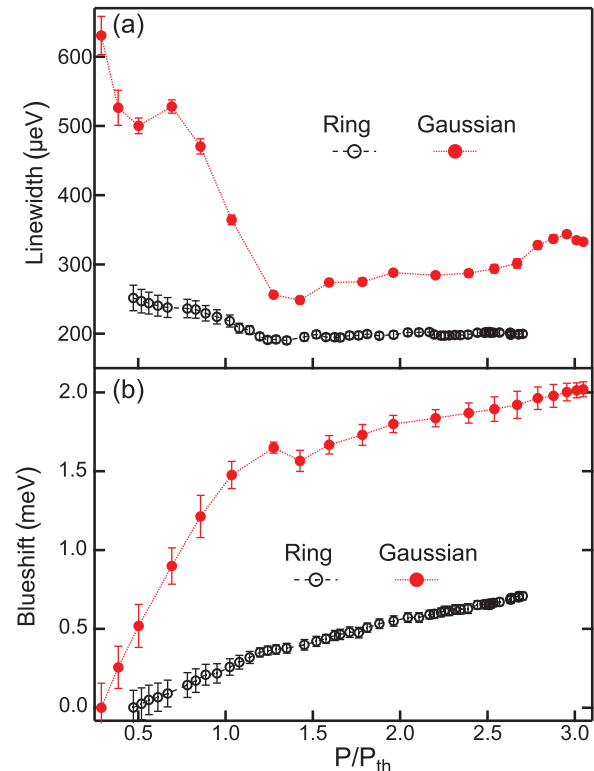


FIG. 5. (Color online) Linewidth and blueshift of polaritons from the center of the ring excitation (open black circles) and from a Gaussian excitation (red circles), measured at $k = 0 \mu\text{m}^{-1}$ of the spatially filtered dispersions. (a) Linewidth vs excitation power for polaritons at the center of the ring and a Gaussian excitation. (b) Energy shift of the two condensates vs threshold power. Lines are guides for the eyes.

interactions.³⁰ Due to the absence of the decoherence mechanisms instigated by the reservoir, in the case of ring excitation, the linewidth is narrower and increases much slower above threshold than in the case of Gaussian excitation. For the optically trapped polaritons the dephasing of the condensate due to the interaction with the exciton reservoir is strongly suppressed.³¹ Thus, above threshold the main mechanism of spectral broadening of the condensate, in the absence of excitons, is governed by polariton-polariton scattering. The linewidth variation of the trapped condensate above threshold is notably small ($\sim 10 \mu\text{eV}$) evidencing that for the power range and detuning (-4 meV) that we examine, the contributions to broadening from polariton self-interactions³² are negligible. Arguably this scales with the polariton exciton fraction.

Interactions with the uncondensed reservoir also affect the energy level of the polaritonic system. The energy shift of the condensate increases linearly with the pumping intensity, for the optically trapped condensate, reflecting the linear increase of the mean number of condensed polaritons [Fig. 5(b)]. In the case of Gaussian excitation, below threshold, the blueshift is strongly affected by the interaction with the reservoir: the increase is four times steeper than in the ring-excitation case while at threshold there is a difference of 1.2 meV .

In conclusion, we have demonstrated the condensation of a polariton bosonic gas in a two-dimensional optical trap.

This configuration allows for the formation of a polariton condensate spatially separated from the excitation area minimizing dephasing and depletion processes associated with the light imprinted excitonic reservoir. As a result, perturbation of the condensate from incoherent particles is greatly suppressed leading to the lowest reported measurement of the Heisenberg uncertainty for polariton condensates. The highly efficient excitation technique of exciton polaritons results in the spontaneous formation of a polariton BEC spatially separated from the excitation laser at more than two times lower excitation densities compared to previous experimental configurations. In the case of a polariton BEC formed through optical trapping, the linewidth reduces and clamps at threshold

clearly evidencing that temporal coherence is not affected by increasing the occupation number of the condensate. Finally, disassociation of the condensate from the excitation beam conclusively settles the debate on the inheritance of coherence of the polariton condensate from the excitation laser.

A.A., A.K., and P.G.L. acknowledge funding from Marie Curie ITN Clermont IV. H.O. and P.G.L. acknowledge funding from EPSRC through Contract No. EP/G063494/1. A.K. acknowledges support from Russian Ministry of Science and Education, Grant No. 11.G34.31.0067 and P.S. acknowledges support from Greek GSRT ARISTEIA program Apollo.

*Author to whom correspondence should be addressed: A.Askitopoulos@soton.ac.uk

¹A. V. Kavokin, J. Baumberg, G. Malpuech, and F. P. Laussy, *Microcavities* (Oxford University Press, Oxford, 2007).

²J. Kasprzak, M. Richard, S. Kundermann, A. Baas, P. Jeambrun, J. M. J. Keeling, F. M. Marchetti, M. H. Szymańska, R. André, J. L. Staehli, V. Savona, P. B. Littlewood, B. Deveaud, and L. S. Dang, *Nature (London)* **443**, 409 (2006).

³R. Balili, V. Hartwell, D. Snoke, L. Pfeiffer, and K. West, *Science* **316**, 1007 (2007).

⁴S. Christopoulos, G. B. H. von Högersthal, A. Grundy, P. G. Lagoudakis, A. V. Kavokin, J. J. Baumberg, G. Christmann, R. Butté, E. Feltin, J.-F. Carlin, and N. Grandjean, *Phys. Rev. Lett.* **98**, 126405 (2007).

⁵G. Nardin, K. G. Lagoudakis, M. Wouters, M. Richard, A. Baas, R. André, L. S. Dang, B. Pietka, and B. Deveaud-Plédran, *Phys. Rev. Lett.* **103**, 256402 (2009).

⁶H. Deng, G. S. Solomon, R. Hey, K. H. Ploog, and Y. Yamamoto, *Phys. Rev. Lett.* **99**, 126403 (2007).

⁷H. Ohadi, E. Kammann, T. C. H. Liew, K. G. Lagoudakis, A. V. Kavokin, and P. G. Lagoudakis, *Phys. Rev. Lett.* **109**, 016404 (2012).

⁸G. Malpuech, Y. G. Rubo, F. P. Laussy, P. Bigenwald, and A. V. Kavokin, *Semicond. Sci. Technol.* **18**, S395 (2003).

⁹R. B. Balili, D. W. Snoke, L. Pfeiffer, and K. West, *Appl. Phys. Lett.* **88**, 031110 (2006).

¹⁰M. Maragkou, A. J. D. Grundy, E. Wertz, A. Lemaître, I. Sagnes, P. Senellart, J. Bloch, and P. G. Lagoudakis, *Phys. Rev. B* **81**, 081307 (2010).

¹¹D. Bajoni, P. Senellart, E. Wertz, I. Sagnes, A. Miard, A. Lemaître, and J. Bloch, *Phys. Rev. Lett.* **100**, 047401 (2008).

¹²L. Ferrier, E. Wertz, R. Johne, D. D. Solnyshkov, P. Senellart, I. Sagnes, A. Lemaître, G. Malpuech, and J. Bloch, *Phys. Rev. Lett.* **106**, 126401 (2011).

¹³A. Das, P. Bhattacharya, J. Heo, A. Banerjee, and W. Guo, *Proc. Natl. Acad. Sci. USA* **110**, 2735 (2013).

¹⁴E. Wertz, L. Ferrier, D. D. Solnyshkov, R. Johne, D. Sanvitto, A. Lemaître, I. Sagnes, R. Grousson, A. V. Kavokin, P. Senellart, G. Malpuech, and J. Bloch, *Nat. Phys.* **6**, 860 (2010).

¹⁵G. Tosi, G. Christmann, N. G. Berloff, P. Tsotsis, T. Gao, Z. Hatzopoulos, P. G. Savvidis, and J. J. Baumberg, *Nat. Phys.* **8**, 190 (2012).

¹⁶T. Gao, P. S. Eldridge, T. C. H. Liew, S. I. Tsintzos, G. Stavrinidis, G. Deligeorgis, Z. Hatzopoulos, and P. G. Savvidis, *Phys. Rev. B* **85**, 235102 (2012).

¹⁷P. Cristofolini, A. Dreismann, G. Christmann, G. Franchetti, N. G. Berloff, P. Tsotsis, Z. Hatzopoulos, P. G. Savvidis, and J. J. Baumberg, *Phys. Rev. Lett.* **110**, 186403 (2013).

¹⁸E. Kammann, H. Ohadi, M. Maragkou, A. V. Kavokin, and P. G. Lagoudakis, *New J. Phys.* **14**, 105003 (2012).

¹⁹H. Deng, G. Weihs, D. Snoke, J. Bloch, and Y. Yamamoto, *Proc. Natl. Acad. Sci. USA* **100**, 15318 (2003).

²⁰P. Tsotsis, P. S. Eldridge, T. Gao, S. I. Tsintzos, Z. Hatzopoulos, and P. G. Savvidis, *New J. Phys.* **14**, 023060 (2012).

²¹See Supplemental Material at <http://link.aps.org/supplemental/10.1103/PhysRevB.88.041308> for experimental setup, further discussion on the trapping mechanism, and the increased scattering efficiency inside the trap and interferometric and energy tomography data.

²²W. Heller, A. Filoramo, P. Roussignol, and U. Bockelmann, *Solid-State Electron.* **40**, 725 (1996).

²³Y. Nagamune, H. Watabe, F. Sogawa, and Y. Arakawa, *Appl. Phys. Lett.* **67**, 1535 (1995).

²⁴M. Gulia, F. Rossi, E. Molinari, P. E. Selbmann, and P. Lugli, *Phys. Rev. B* **55**, R16049 (1997).

²⁵E. Kammann, T. C. H. Liew, H. Ohadi, P. Cilibrizzi, P. Tsotsis, Z. Hatzopoulos, P. G. Savvidis, A. V. Kavokin, and P. G. Lagoudakis, *Phys. Rev. Lett.* **109**, 036404 (2012).

²⁶P. G. Savvidis, J. J. Baumberg, R. M. Stevenson, M. S. Skolnick, D. M. Whittaker, and J. S. Roberts, *Phys. Rev. Lett.* **84**, 1547 (2000).

²⁷G. Roumpos, W. H. Nitsche, S. Höfling, A. Forchel, and Y. Yamamoto, *Phys. Rev. Lett.* **104**, 126403 (2010).

²⁸S. Utsunomiya, L. Tian, G. Roumpos, C. W. Lai, N. Kumada, T. Fujisawa, M. Kuwata-Gonokami, A. Löffler, S. Höfling, A. Forchel, and Y. Yamamoto, *Nat. Phys.* **4**, 700 (2008).

²⁹D. V. Vishnevsky, D. D. Solnyshkov, N. A. Gippius, and G. Malpuech, *Phys. Rev. B* **85**, 155328 (2012).

³⁰A. P. D. Love, D. N. Krizhanovskii, D. M. Whittaker, R. Bouchekioua, D. Sanvitto, S. A. Rizeiqi, R. Bradley, M. S. Skolnick, P. R. Eastham, R. André, and L. S. Dang, *Phys. Rev. Lett.* **101**, 067404 (2008).

³¹F. Tassone and Y. Yamamoto, *Phys. Rev. A* **62**, 063809 (2000).

³²D. Porras and C. Tejedor, *Phys. Rev. B* **67**, 161310 (2003).